Theoretical Chemistry Accounts (2018) 137:76
https://doi.org/10.1007/s00214-018-2251-y

REGULAR ARTICLE

Reactivity of chlorogenic acid toward hydroxyl and methyl peroxy radicals relative to trolox in nonpolar media

Jelena Tošović[1] · **Svetlana Marković**[1]

Received: 14 March 2018 / Accepted: 23 April 2018 / Published online: 8 May 2018

Abstract

The quantum mechanics-based test for overall free-radical scavenging activity was applied for the investigation of antioxidative capacity of chlorogenic acid (5-*O*-caffeoylquinic acid, **5CQA**) relative to trolox (6-hydroxy-2,5,7,8-tetramethylchroman-2-carboxylic acid, **Tx**) as a reference compound. Hydrogen atom transfer (HAT), radical adduct formation (RAF), electron transfer (**ET**), and proton loss (**PL**) reactions of **5CQA** and **Tx** with $HO^{\bullet}$ and $CH_3OO^{\bullet}$ radicals in benzene and pentyl ethanoate were examined. For this purpose, two theoretical models, M06-2X/6-311++G(d,p) in combination with the CPCM solvation model, and M05-2X/6-311++G(d,p) in combination with the SMD solvation model, were employed. It was found that M05-2X/6-311++G(d,p)—SMD failed to evaluate the influence of pentyl ethanoate, whereas M06-2X—CPCM in benzene and pentyl ethanoate and M05-2X—SMD in benzene proved to be operative and showed similar trends. Both compounds can react with $HO^{\bullet}$ via HAT and RAF mechanisms, whereas HAT is the only reaction pathway with $CH_3OO^{\bullet}$. **5CQA** is more efficient scavenger of $HO^{\bullet}$ than **Tx**, but less efficient scavenger of $CH_3OO^{\bullet}$. Less reactive free radicals are more suitable for the determination of antioxidative activity of a compound relative to **Tx**. Highly reactive free radicals need to be included in the investigation of all potential reaction pathways of the compound, in which case the results from different approaches can be inconsistent.

Keywords Antioxidative activity · Rate constants · r^T values · M06-2X/6-311++G(d,p)—CPCM · M05-2X/6-311++G(d,p)—SMD

1 Introduction

Highly reactive free radicals, such as hydroxyl and peroxyl radicals, are produced in the organism during normal metabolic processes. Imbalance between formation and consumption of free radicals leads to phenomenon known as oxidative stress [1]. These reactive species contribute to oxidative damage to proteins, DNA and lipids and are associated with some diseases [2, 3]. Thus, the compounds able to scavenge free radicals are in the focus of contemporary investigations. Numerous epidemiological studies have shown that dietary antioxidants can reduce development and progression of some chronic diseases [4–7]. One of the most abundant phenolic acid antioxidants present in fruits and vegetables is chlorogenic acid (5-*O*-caffeoylquinic acid, **5CQA**) (Fig. 1) [8].

A wide range of experimental assays are used to evaluate antioxidative capacity [9–12]. Roughly, there are two types of these assays: chemical and biological [13]. In biological assays the damage in biomolecules caused by radical processes is measured. Chemical assays are used in studies which are devoted to evaluation of the rate constants for the reactions between free radicals and antioxidants. In these assays the antioxidative capacity of a compound is compared to that of some reference compound. The most commonly used antioxidant for this purpose is trolox (6-hydroxy-2,5,7,8-tetramethylchroman-2-carboxylic acid, **Tx**) (Fig. 2).

Recently, a computational protocol known as the quantum mechanics-based test for overall free-radical scavenging activity (QMORSA) has been proposed for estimating antioxidative capacity of compound [14]. This approach is based

Electronic supplementary material The online version of this article (https://doi.org/10.1007/s00214-018-2251-y) contains supplementary material, which is available to authorized users.

✉ Jelena Tošović
jelena.tosovic@pmf.kg.ac.rs

[1] Faculty of Science, University of Kragujevac, 12 Radoja Domanovića, Kragujevac 34000, Serbia

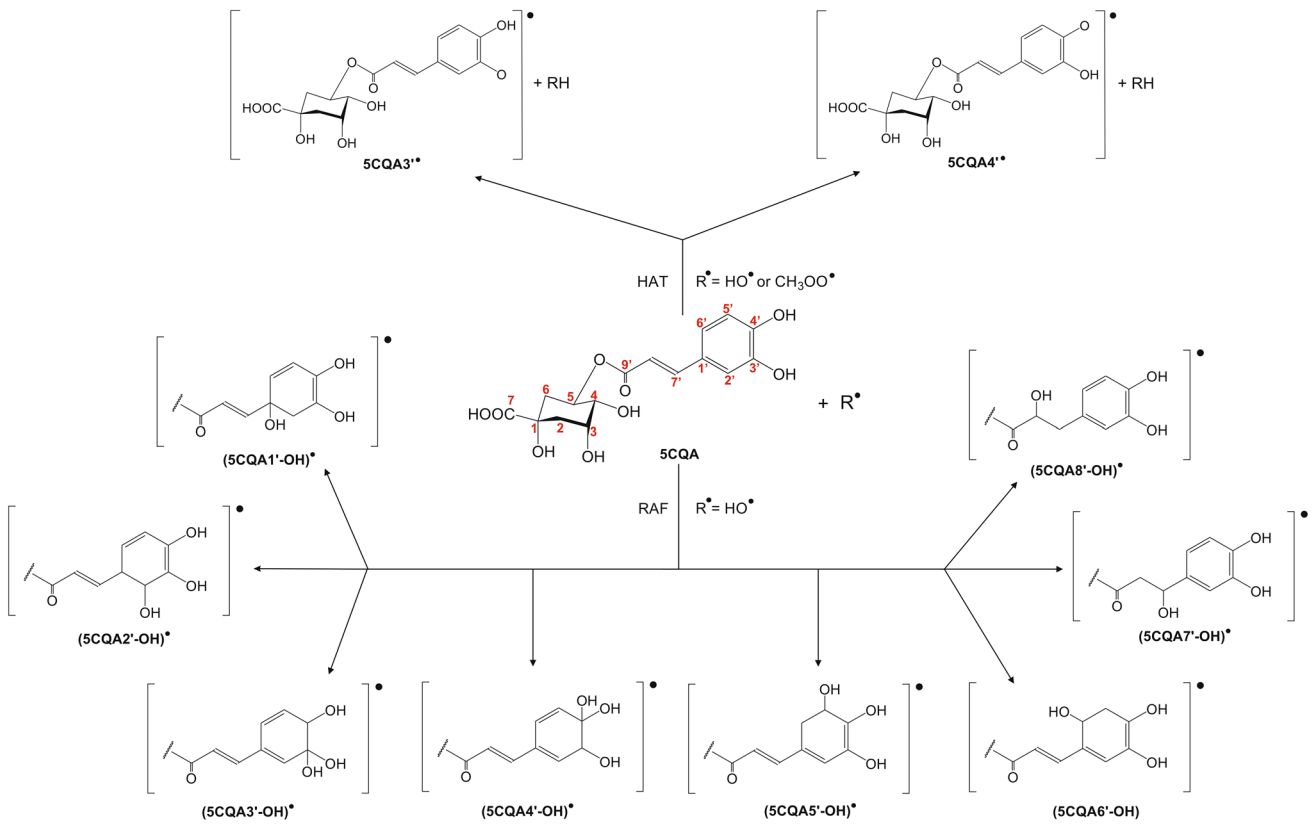

Fig. 1 Possible antioxidative reaction pathways of **5CQA** in nonpolar solvents. The atoms labeling scheme and product names are indicated

on thermodynamic and kinetic investigation of all possible reactions included in antioxidative processes for examined compound. Namely, this methodology requires calculation of rate constants for all probable mechanistic pathways of an antioxidant in media of different polarity considering the influence of pH. Like experimental studies, this approach also offers possibility for determination of the relative antioxidative activity using **Tx** as a reference antioxidant. Thus, the ratio between overall rate constants of examined antioxidant and **Tx** can indicate larger or smaller activity of the antioxidant in comparison to **Tx**.

There are several theoretical studies devoted to explanation of antioxidative action of **5CQA** [15–19] including thermodynamic and mechanistic approaches to the hydrogen atom transfer (HAT), radical adduct formation (RAF), sequential proton loss–electron transfer (SPLET), and single electron transfer–proton transfer (SET-PT) mechanisms. In our recent paper [17], kinetic investigations of the four mechanisms of **5CQA** with $HO^{\bullet}$ have revealed that in neutral and acidic media HAT and RAF mechanisms are competitive, whereas in basis media (e.g., at physiological pH) SPLET mechanism is predominant.

This work is an extension of our efforts aimed at elucidation of antioxidative properties of **5CQA**. The goal of the work is to determine relative antioxidative capacity of **5CQA** using **Tx** as a reference (r^{T}) in nonpolar solvents. For this purpose, all antioxidative pathways of **5CQA** and **Tx** with two free radicals, $HO^{\bullet}$ (extremely reactive) and $CH_3OO^{\bullet}$ (moderately reactive), were investigated by means of two theoretical models. An additional goal is to examine the performances of the applied theoretical models in evaluation of the r^{T} values of **5CQA**.

2 Computational details

Within this work all calculations were performed using the Gaussian 09 program package [20]. Two levels of theory were applied: M06-2X/6-311++G(d,p) [21, 22] in combination with the CPCM polarizable continuum solvation model [23] and M05-2X/6-311++G(d,p) [24] in combination with the SMD continuum solvation model [25]. The former theoretical model has recently demonstrated robustness and very good overall performance in investigations of the related problems [15, 17, 21, 26], where it was applied in a manner that the influence of solvent to the structure and energy was estimated by full geometry optimizations, including frequency calculations. The latter density functional and solvation model have often been employed [27–31]. Sometimes, their application was based on the gas-phase calculations

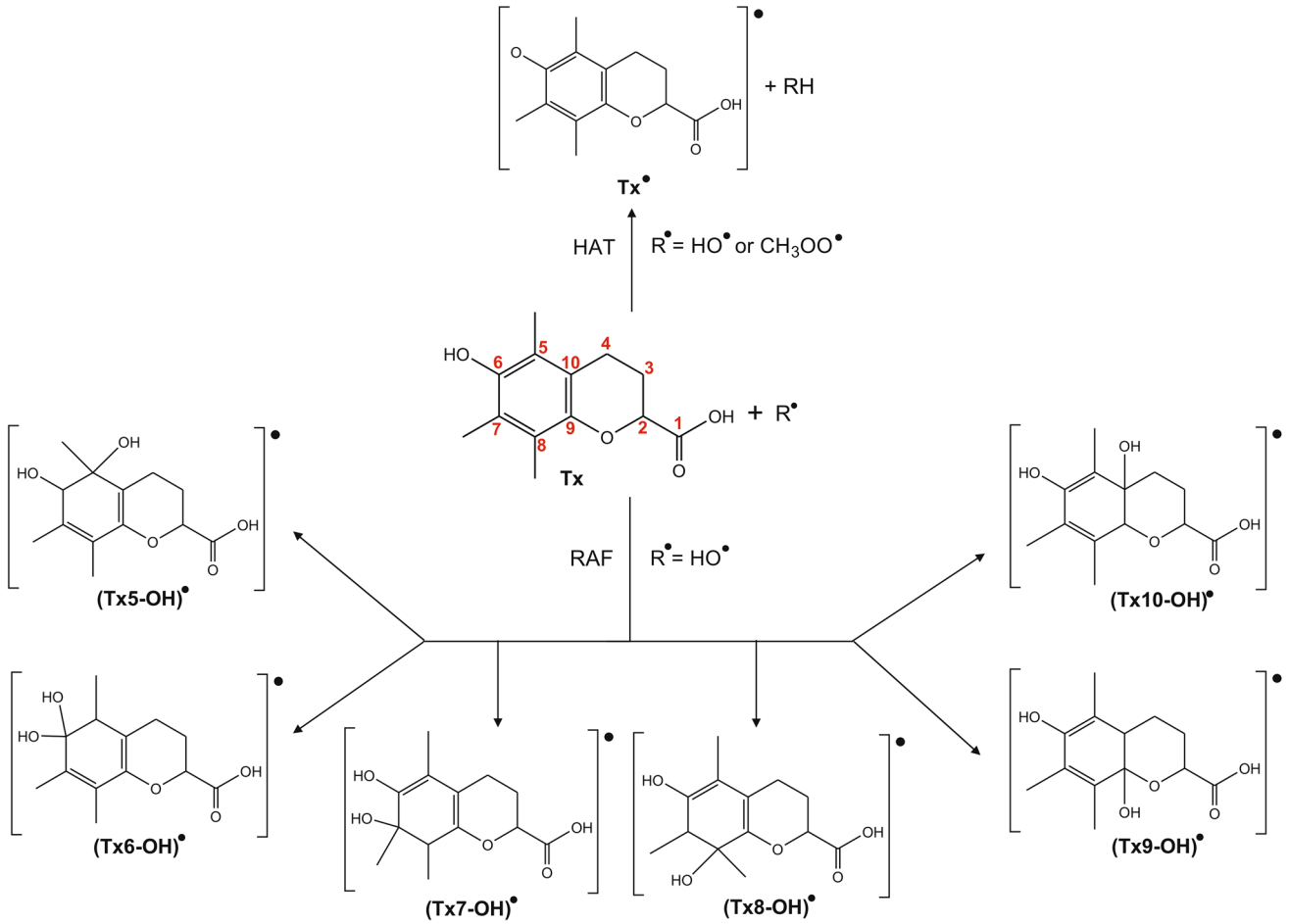

Fig. 2 Possible antioxidative reaction pathways of **Tx** in nonpolar solvents. The atoms labeling scheme and product names are indicated

[27, 29], and the solvent cage effects were included according to the corrections proposed by Okuno [32] taking into account the free volume theory [33].

Following our strategy (full optimizations with frequency calculations included) we performed the calculations taking into account the effects of two solvents of similar polarity: benzene (dielectric constant $\varepsilon = 2.2706$) and pentyl ethanoate ($\varepsilon = 4.7297$). The restricted and unrestricted calculation schemes were applied for the closed-shell and open-shell structures. The nature of the revealed stationary points was determined by analyzing the results of the frequency calculations: no imaginary vibrations for equilibrium geometries and exactly one imaginary vibration for transition states. The intrinsic reaction coordinate (IRC) calculations were carried out to confirm that each transition state connects two corresponding equilibrium geometries.

The following reactions were considered:

$$\text{Phenolic} + \text{R}^{\cdot} \rightarrow \text{Phenolic}^{\cdot} + \text{RH} \quad (1)$$

$$\text{Phenolic} + \text{R}^{\cdot} \rightarrow (\text{Phenolic} - \text{R})^{\cdot} \quad (2)$$

$$\text{Phenolic} \rightleftarrows \text{Phenolic}^{-} + \text{H}^{+} \quad (3)$$

$$\text{Phenolic} + \text{R}^{\cdot} \rightleftarrows \text{Phenolic}^{+\cdot} + \text{R}^{-} \quad (4)$$

In Eqs. (1)–(4) Phenolic stands for **5CQA** and **Tx**, whereas $\text{R}^{\bullet}$ denotes the $\text{HO}^{\bullet}$ and $\text{CH}_3\text{OO}^{\bullet}$ radicals. Accordingly, $\text{Phenolic}^{\bullet}$, $(\text{Phenolic-R})^{\bullet}$, Phenolic^{-}, and $\text{Phenolic}^{+\bullet}$ represent the free radical, radical adduct, anion, and radical cation issued from the corresponding phenolic compound, respectively. Apparently, RH is the parent compound of $\text{R}^{\bullet}$, and R^{-} is the corresponding anion. The $\text{HO}^{\bullet}$ radical is produced during Fenton and Haber–Weiss reactions in organism and represents one of the most potent radicals of biological importance. $\text{CH}_3\text{OO}^{\bullet}$ radical is selected to imitate behavior of larger lipid peroxide radicals. Equations (1) and (2) represent the HAT and RAF mechanisms. Equations (3) and (4) characterize the first steps of the SPLET (proton loss) and SET-PT (electron transfer) mechanisms. The free energies of the reactions at $T = 298.15$ K in the two solvents were determined. The free energy values of the solvated proton

[Eq. (3)] in benzene (−901.8 kJ mol^{-1}) and pentyl ethanoate (−1015.5 kJ mol^{-1}) were taken from the literature [34].

The rate constants were calculated for 1 M standard state using the Eckart method, also known as ZCT-0 [35]:

$$k_{\mathrm{ZCT-0}} = \sigma\gamma(T)\frac{k_{\mathrm{B}}T}{h}\exp\left(-\Delta G_a^{\ddagger}/RT\right) \quad (5)$$

For this purpose TheRate program was utilized [36]. In Eq. (5) k_{B} and h stand for the Boltzman and Planck constants, whereas $\Delta G_a^{\ddagger}$, σ, and $\gamma(T)$ are the free activation energy, reaction path degeneracy, and transmission coefficient, respectively [37]. The energy values and partition functions were taken from the quantum mechanical calculations.

Each k_{overall} value was obtained as a sum of the corresponding $k_{\mathrm{ZCT-0}}$ values. The r^{T} (antioxidative activity of **5CQA** relative to **Tx**) value was calculated by dividing k_{overall} for **5CQA** with k_{overall} for **Tx** at three different levels of theory. The branching ratio, i.e., the percent contribution of an antioxidative pathway i to the overall reaction of **5CQA**, was calculated by dividing $k_{\mathrm{ZCT-0}}(i)$ with k_{overall} and multiplying with 100.

3 Results and discussion

The first part of our investigation was devoted to thermodynamic consideration of the reactions (1)–(4). The aim of this examination was to select exergonic reaction pathways for further analysis. Bearing in mind that the rate constants for homolytic cleavage of the C–H bonds and corresponding branching ratios are much smaller in comparison to those for homolytic cleavage of the O–H bonds [27, 29, 38–40], examination of the HAT mechanism was focused to abstraction of hydrogen atoms from phenolic groups. As for the RAF mechanism, addition of the two free radicals to the sp^2 hybridized carbon atoms was simulated. The results are presented in Table 1 and illustrated with Figs. 1 and 2. It is apparent that the $\Delta_r G$ values refereeing to the two solvents are in very good agreement. As expected for nonpolar solvents, both compounds show pronouncedly positive $\Delta_r G$ values for the loss of carboxylic proton [Eq. (3)] and for the transfer of electron to either HO$^{\bullet}$ or $CH_3OO^{\bullet}$ [Eq. (4)]. In accordance with previous findings [15–18, 38], these results show that neither **5CQA** nor **Tx** undergo the SPLET and SET-PT mechanisms in nonpolar media. For this reason the further steps of these antioxidative pathways were not examined, and they were excluded from the text that follows.

On the other hand, HAT is thermodynamically favorable mechanism of **5CQA** and **Tx** with both free radicals, where the reactions with HO$^{\bullet}$ are noticeably more exergonic. In addition, the $\Delta_r G$ values for the RAF pathways with HO$^{\bullet}$ are in most cases negative, except for the positions 9' of **5CQA** and 1 of **Tx** (Table 1). Certainly, these positions are not attractive for highly electrophilic HO$^{\bullet}$ because of the large partial positive charge on C9′ of **5CQA** and C1 of **Tx**. All RAF pathways of both phenolics with $CH_3OO^{\bullet}$ are endergonic, which can mainly be attributed to significantly lower reactivity of this free radical, and, to some extent, to its voluminosity. The products of all exergonic HAT and RAF pathways are presented in Figs. 1 (those related to **5CQA**) and 2 (those related to **Tx**).

All these exergonic reaction pathways were subjected to kinetic investigation, aimed at revealing the transition states and calculating the corresponding rate constants and r^{T} values. The located transition states for the antioxidative pathways of **5CQA** and **Tx** are depicted in Figs. 3 and 4, whereas the activation energies, as well as the $k_{\mathrm{ZCT-0}}$ and r^{T} values related to both solvents, are collected in Table 2. Two examples of the IRC calculations for **5CQA** with HO$^{\bullet}$ in benzene are presented in Figs S1 and S2. Also, representative examples, including appropriate discussion, for dependence of rate constants on temperature for both **5CQA** and **Tx** are depicted in Figs S3 and S4, respectively.

It is well known that HAT and RAF only slightly depend on solvent polarity [15–17, 26, 31, 41]. For example, it can be easily calculated from the results presented in Ref. [17] that k_{overall} for the reaction of **5CQA** with HO$^{\bullet}$ in polar solvents, ethanol, and water amounts to 9.46×10^8 and 9.60×10^8 (the same order of magnitude as k_{overall} for the reaction in benzene). Since benzene and pentyl ethanoate are of comparable polarity, it is reasonable to expect that the k_{overall} and r^{T} values for a certain free radical will be very similar. Table 2 shows that the r^{T} values for $CH_3OO^{\bullet}$ are almost identical. To our surprise, r^{T} for HO$^{\bullet}$ is much larger in pentyl ethanoate than in benzene. To clarify this unexpected finding, we performed additional investigation. Actually, we repeated all calculations related to the kinetics of the HAT and RAF pathways of **5CQA** and **Tx** using the M05-2X/6-311++G(d,p) level of theory in combination with the SMD solvation model. It should be pointed out that all necessary structures and corresponding free energies were obtained by full optimizations and frequency calculations. The results obtained are presented in Table 3.

It is worth emphasizing that M05-2X/6-311++G(d,p) in conjunction with SMD was not able to locate the majority of transition states for the HAT pathways of **5CQA** in pentyl ethanoate. In these cases geometry convergence could not be achieved, which is illustrated with Fig S5. Thus, this level of theory could not produce either the k_{overall} values of **5CQA** in pentyl ethanoate, or the corresponding r^{T} values for both free radicals. On the other hand, all reaction pathways in benzene were revealed, and the corresponding k_{overall} and r^{T} values were calculated. Thus, we can compare three sets of results in Tables 2 and 3 and calculate three sets of branching ratios (Table 4).

Table 1 Gibbs energies (kJ mol^{-1}) of the reactions (1)–(4) for chlorogenic acid (**5CQA**) and trolox (**Tx**) calculated at the M06-2X/6-311++G(d,p) level of theory in combination with the CPCM solvation model

Mechanism	Position	5CQA		Tx		
		$HO^{\bullet}$	$CH_3OO^{\bullet}$	Position	$HO^{\bullet}$	$CH_3OO^{\bullet}$
Benzene						
HAT	3′	−150.7[a]	−9.2			
	4′	−160.5[a]	−18.9	6	−167.2	−25.7
RAF	1′	−18.2	104.2			
	2′	−53.0	66.8	1	25.7	166.5
	3′	−37.9	84.6	5	−59.7	61.5
	4′	−77.3	52.1	6	−60.1	60.7
	5′	−33.7	83.1	7	−43.5	74.9
	6′	−55.6	65.6	8	−50.0	87.5
	7′	−81.8[a]	37.0	9	−41.4	77.0
	8′	−101.8[a]	23.9	10	−35.0	84.3
	9′	24.6	150.1			
PL	1	339.4		1	374.1	
ET	/	339.4[a]	418.8	/	260.1	339.5
Pentyl ethanoate						
HAT	3′	−151.9	−8.8			
	4′	−161.4	−18.3	6	−169.1	−26.0
RAF	1′	−16.1	106.2			
	2′	−51.2	69.6	1	32.2	168.2
	3′	−37.1	86.1	5	−54.0	65.2
	4′	−75.5	53.9	6	−57.3	63.7
	5′	−30.0	87.7	7	−41.1	77.1
	6′	−54.6	66.5	8	−48.0	88.1
	7′	−80.5	38.4	9	−39.4	79.5
	8′	−99.9	25.2	10	−29.8	86.1
	9′	25.9	151.0			
PL	1	182.0		1	209.5	
ET	/	217.7	306.6	/	150.6	239.5

PL (proton loss) and ET (electron transfer) denote the first steps of the SPLET and SET-PT mechanisms. See Figs. 1 and 2 for the atoms labeling scheme

[a]The free energy values were taken from Ref. [17]

Analysis of the results presented in Tables 2, 3 and 4 shows that, despite numerical differences, all three operative computational methodologies, M06-2X—CPCM in benzene and pentyl ethanoate, and M05-2X—SMD in benzene (with the same basis set), exhibit similar trends. In nonpolar solvents the two antioxidants undergo both HAT and RAF pathways with $HO^{\bullet}$, and only HAT mechanism with $CH_3OO^{\bullet}$. As for the reactions of both phenolics with $HO^{\bullet}$, the RAF pathways are generally faster. The fastest pathways of **5CQA** and **Tx** are RAFs in the positions 4′ and 6, respectively. A common feature of TS4′ and TS6 (Figs. 3, 4) is that both transition states are stabilized with hydrogen bonds between approaching $HO^{\bullet}$ and phenolic groups and, thus, require low activation energies. On the other hand, attractive interactions in the HAT reaction paths [hydrogen bond between the oxygen of the hydroxyl moiety and proximate phenolic group in TS3′($HO^{\bullet}$) and TS4′($HO^{\bullet}$) and π-interactions between the hydrogen of the hydroxyl moiety and aromatic ring in TS($HO^{\bullet}$)] slow down the formation of hydrogen peroxide and its leaving the reaction system. Thus, despite the finding that addition of $HO^{\bullet}$ to the double bond of **5CQA** is thermodynamically most favorable (Table 1), the greatest Γ value for the reaction of **5CQA** with $HO^{\bullet}$ comes from the RAF pathway in the 4′ position. As for the HAT pathways

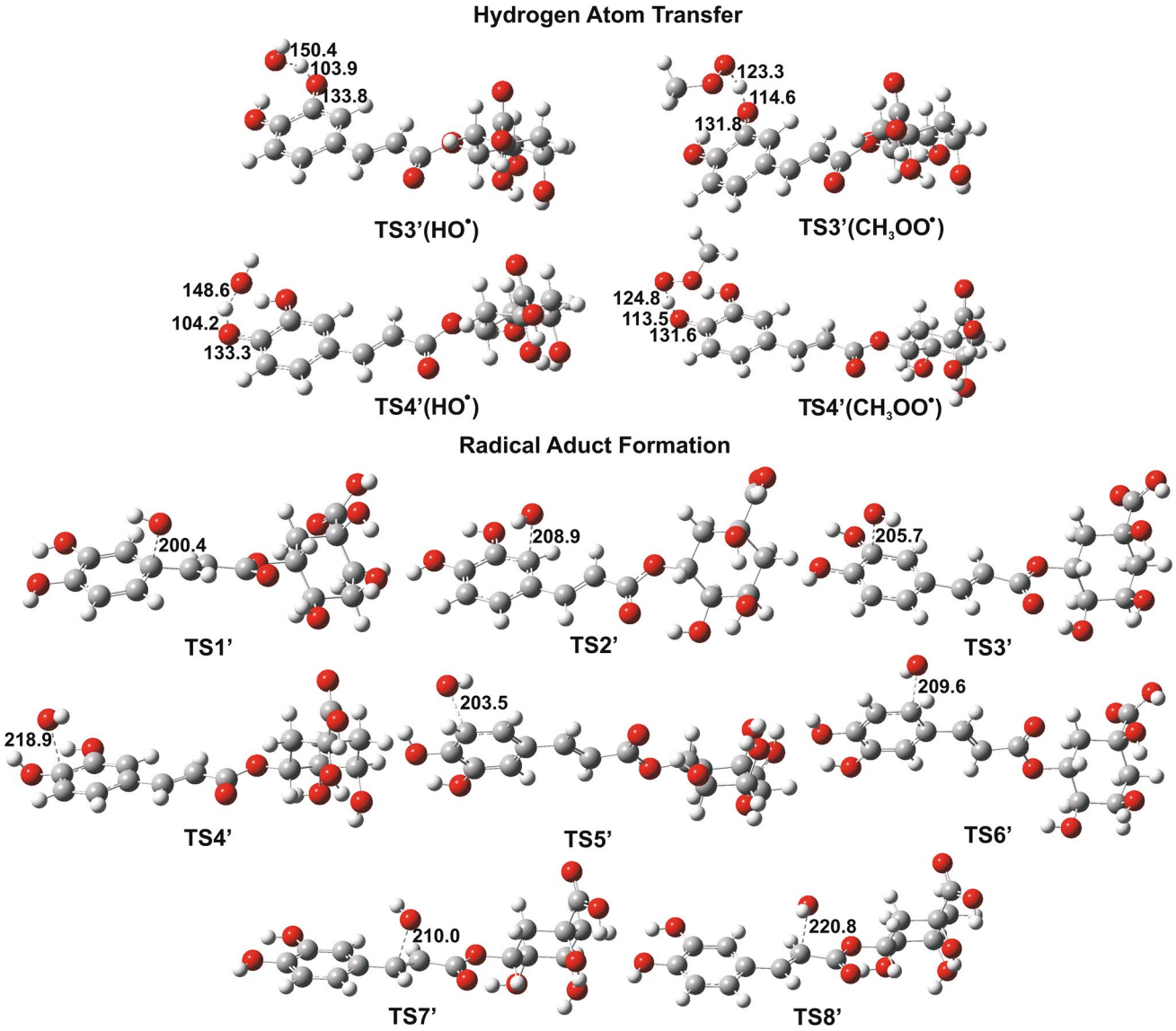

Fig. 3 Optimized geometries of transition states figuring in the reactions of **5CQA** with HO• and CH_3OO• in benzene. The key bond distances are given in Å. The calculations were performed at the M06-2X/6-311++G(d,p) level of theory in combination with the CPCM solvation model

with CH_3OO•, the Γ values for the 4′ position are larger, and in case of the SMD solvation model the difference between the branching ratios is distinct.

5CQA is more reactive toward HO• than **Tx** ($r^T > 1$), but less reactive toward CH_3OO• ($r^T < 1$). Larger reactivity of **5CQA** toward HO• is mainly a consequence of very fast RAF pathways. In comparison to **Tx**, **5CQA** has more suitable positions for addition of HO•. Furthermore, the RAF pathway in the 4′ position of **5CQA** is the fastest reaction path according to all three operative methodologies. The r^T values for CH_3OO• are mutually very similar, while those for HO• differ, where r^T in pentyl ethanoate particularly deviates (Tables 2 and 3). Such behavior of r^T for HO• is probably a consequence of extreme reactivity of this radical that is challenging to be numerically evaluated, whatever computational methodology is used. Thus, it is more practical to use less reactive free radicals in tasks devoted to determination of antioxidative activity of some compound relative to **Tx** [14,

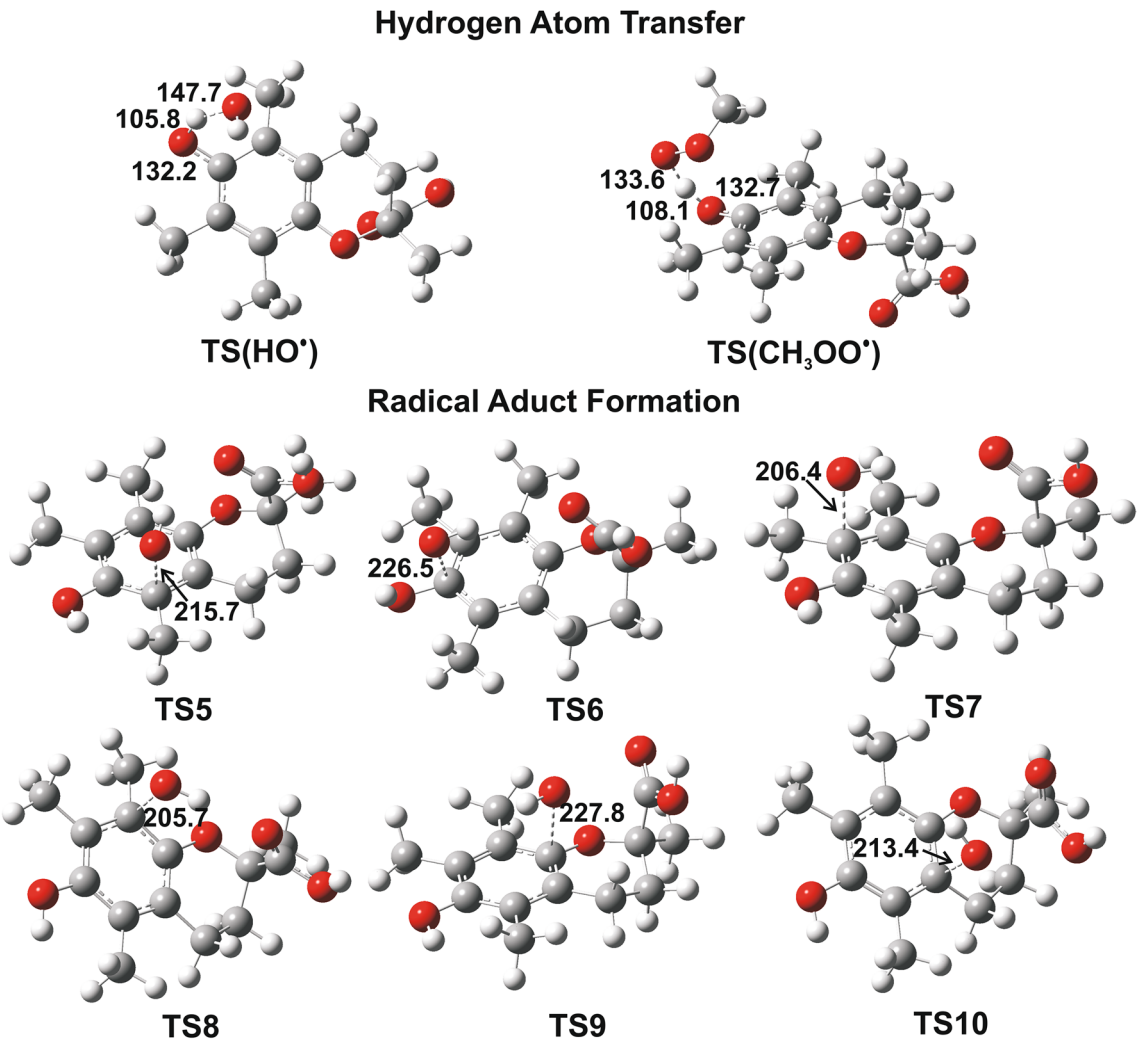

Fig. 4 Optimized geometries of transition states figuring in the reactions of **Tx** with HO• and CH_3OO• in benzene. The key bond distances are given in Å. The calculations were performed at the M06-2X/6-311++G(d,p) level of theory in combination with the CPCM solvation model

42, 43]. However, if one's goal is to examine all possible antioxidative pathways of the compound, they need to use highly reactive free radicals.

The reactions of **5CQA** with two simple free radicals in pentyl ethanoate indicate disadvantage of the combination of the M05-2X functional and SMD solvation model to accomplish some routine computational tasks, such as finding energy maxima. On the other hand, the $k_{overall}$ values related to the reaction of **Tx** with both free radicals were obtained in this way and are mutually comparable (Tables 2, 3). Now we can compare the rate constants and $k_{overall}$ related to the reactions with HO• obtained in this work (Table 3) to those presented in Ref. [38]. General impression is that the values presented here are by two orders of magnitude smaller than those suggested by Alberto et al. [38]. The most noteworthy difference is that we revealed a reaction path for homolytic cleavage of the O–H bond of the phenolic group and calculated the rate constant of 5.54×10^6 M^{-1} s^{-1}, whereas Alberto et al. found that this process is diffusion controlled and assigned it the rate constant of 1.91×10^9 M^{-1} s^{-1}. Inconsistency between the two sets of results is, certainly, a consequence of already explained difference in applied computational methodology. We approve the approach based on geometry optimization and frequency calculation

Table 2 Gibbs energies of activation $\Delta G_a^{\ddagger}$ (kJ mol^{-1}) and rate constants $k_{ZCT\text{-}0}$ (M^{-1} s^{-1}) for the HAT and RAF reactions of **5CQA** and **Tx** with HO$^{\bullet}$ and $CH_3OO^{\bullet}$ radicals. The results were produced at the M06-2X/6-311++G(d,p) level of theory in combination with the CPCM solvation model

Compound		5CQA				Tx				
Radical		HO$^{\bullet}$		$CH_3OO^{\bullet}$		HO$^{\bullet}$			$CH_3OO^{\bullet}$	
		$\Delta G_a^{\ddagger}$	$k_{ZCT\text{-}0}$	$\Delta G_a^{\ddagger}$	$k_{ZCT\text{-}0}$		$\Delta G_a^{\ddagger}$	$k_{ZCT\text{-}0}$	$\Delta G_a^{\ddagger}$	$k_{ZCT\text{-}0}$
Benzene										
HAT	3′	41.5[a]	1.61×10^{7}[a]	70.9	2.47×10^{3}					
	4′	45.5[a]	4.54×10^{6}[a]	69.3	3.49×10^{3}	6	25.3	6.49×10^{6}	57.1	4.17×10^{4}
RAF	1′	52.7[a]	1.21×10^{5}[a]			5	18.5	1.33×10^{7}		
	2′	36.8[a]	2.89×10^{7}[a]			6	12.6	5.86×10^{7}		
	3′	40.3[a]	1.55×10^{7}[a]			7	30.7	7.46×10^{6}		
	4′	26.5[a]	8.44×10^{7}[a]			8	28.4	4.48×10^{6}		
	5′	36.9[a]	3.73×10^{7}[a]			9	30.5	2.03×10^{7}		
	6′	36.6[a]	6.82×10^{7}[a]			10	28.4	2.05×10^{7}		
	7′	39.9[a]	1.94×10^{7}[a]							
	8′	25.4[a]	5.82×10^{7}[a]							
$k_{overall}$			3.33×10^{8}		5.96×10^{3}			1.31×10^{8}		4.17×10^{4}
r^T			2.5		0.14					
Pentyl ethanoate										
HAT	3′	43.2	9.35×10^{6}	73.4	1.53×10^{3}					
	4′	47.1	2.46×10^{6}	72.3	1.75×10^{3}	6	27.0	7.05×10^{6}	59.4	2.47×10^{4}
RAF	1′	52.6	1.21×10^{5}							
	2′	35.9	5.87×10^{7}			5	23.3	6.42×10^{6}		
	3′	40.0	1.81×10^{7}			6	19.3	2.83×10^{7}		
	4′	27.7	8.43×10^{8}			7	31.0	6.21×10^{6}		
	5′	38.3	3.73×10^{7}			8	28.4	3.24×10^{6}		
	6′	33.9	1.97×10^{8}			9	29.2	4.31×10^{7}		
	7′	38.9	2.78×10^{7}			10	32.3	1.29×10^{7}		
	8′	24.5	9.01×10^{7}							
$k_{overall}$			1.28×10^{9}		3.28×10^{3}			9.43×10^{7}		2.47×10^{4}
r^T			13.6		0.13					

[a] The free energy values were taken from Ref. [17]

r^T denotes the antioxidative activity of **5CQA** relative to **Tx**

in conjunction with some continuum solvation model, as such tasks are nowadays routine.

A logical next step of our investigation is to determine r^T of **5CQA** in water. In slightly basic aqueous solution **5CQA** exists in the form of monoanion and dianion. Extremely complex behavior of these species toward free radicals is under our intense scrutiny.

4 Summary

The quantum mechanics-based test for overall free-radical scavenging activity (QMORSA) is a very useful computational protocol for estimating r^T of a compound, i.e., its antioxidative activity relative to some reference compound, usually **Tx** [14]. It is practical that QMORSA calculations are conducted by using a unique approach, so that the results of different investigations can be mutually compared. In this work we evaluated the r^T values of **5CQA** for the HO$^{\bullet}$ and $CH_3OO^{\bullet}$ radicals in two nonpolar solvents by applying two different methodologies. It turned out that repeatedly suggested M05-2X functional in conjunction with the SMD

Table 3 Gibbs energies of activation $\Delta G_a^{\ddagger}$ (kJ mol^{-1}) and rate constants $k_{ZCT\text{-}0}$ (M^{-1} s^{-1}) for the HAT and RAF reactions of **5CQA** and **Tx** with HO$^{\bullet}$ and $CH_3OO^{\bullet}$ radicals. The results were produced at the M05-2X/6-311++G(d,p) level of theory in combination with the SMD solvation model

Compound		5CQA					Tx				
Radical		HO$^{\bullet}$			$CH_3OO^{\bullet}$		HO$^{\bullet}$			$CH_3OO^{\bullet}$	
		$\Delta G_a^{\ddagger}$	$k_{ZCT\text{-}0}$		$\Delta G_a^{\ddagger}$	$k_{ZCT\text{-}0}$		$\Delta G_a^{\ddagger}$	$k_{ZCT\text{-}0}$	$\Delta G_a^{\ddagger}$	$k_{ZCT\text{-}0}$
Benzene											
HAT	3′	43.3	8.01×10^{6}		76.7	3.29×10^{2}					
	4′	42.7	1.27×10^{7}		70.5	2.60×10^{3}	6	17.1	1.29×10^{7}	60.4	2.78×10^{4}
RAF	1′	52.8	1.17×10^{5}								
	2′	36.4	4.39×10^{7}				5	16.8	5.03×10^{7}		
	3′	41.2	1.08×10^{7}				6	12.5	1.24×10^{8}		
	4′	23.6	2.64×10^{8}				7	30.3	2.30×10^{7}		
	5′	35.0	2.49×10^{7}				8	28.0	1.69×10^{7}		
	6′	38.9	2.81×10^{7}				9	36.4	2.76×10^{7}		
	7′	39.9	1.94×10^{7}				10	30.5	3.25×10^{7}		
	8′	25.7	5.50×10^{7}								
$k_{overall}$			4.67×10^{8}			2.93×10^{3}			2.87×10^{8}		2.78×10^{4}
r^{T}			1.63			0.11					
Pentyl ethanoate											
HAT	3′	/	/		/	/	6	24.0	5.54×10^{6}	68.0	2.39×10^{3}
	4′	46.6	2.81×10^{6}		/	/					
RAF	1′	52.7	1.20×10^{5}				5	23.2	2.03×10^{7}		
	2′	37.7	3.75×10^{7}				6	18.9	7.00×10^{7}		
	3′	40.0	1.75×10^{7}				7	34.3	8.71×10^{6}		
	4′	29.3	1.27×10^{8}				8	30.4	7.74×10^{6}		
	5′	38.5	3.09×10^{7}				9	37.0	5.40×10^{7}		
	6′	37.7	4.69×10^{7}				10	35.7	2.14×10^{7}		
	7′	40.1	1.78×10^{7}								
	8′	25.0	7.09×10^{7}								
$k_{overall}$			/			/			1.88×10^{8}		2.39×10^{3}
r^{T}			/			/					

r^{T} denotes the antioxidative activity of **5CQA** relative to **Tx**

solvation model failed to estimate the influence of pentyl ethanoate, selected to mimic lipid environment, because of unusual convergence failures. This finding is quite unexpected since SMD employs a set of parameters optimized over the M05-2X/MIDI!6D, M05-2X/6-31G(d), M05-2X/6-31+G(d,p), M05-2X/cc-pVTZ, B3LYP/6-31G(d), and HF/6-31G(d) theoretical methods [25]. On the other hand, other three methodologies, M06-2X—CPCM in benzene and pentyl ethanoate and M05-2X—SMD in benzene, proved to be operative and showed similar trends. Namely, **5CQA** and **Tx** undergo both HAT and RAF paths with HO$^{\bullet}$, and only HAT path with $CH_3OO^{\bullet}$, where **5CQA** is more reactive toward HO$^{\bullet}$ than **Tx**, but less reactive toward $CH_3OO^{\bullet}$. Discrepancy of the results related to HO$^{\bullet}$, particularly in pentyl ethanoate, can be attributed to general inability of computational methodologies to numerically evaluate extreme reactivity of this radical.

Our research confirms that if one's goal is to determine antioxidative activity of a compound relative to **Tx**, it is more useful to include less reactive free radicals in investigation [14, 42, 43]. However, if one's goal is to examine all possible antioxidative pathways of the compound, it is necessary to employ highly reactive free radicals, and in such case different approaches can lead to inconsistent results.

As a final point, which approach should be applied in investigations of antioxidative activity? We strongly suggest the approach based on geometry optimization and frequency calculation in conjunction with continuum

Table 4 Branching ratios (Γ) for all favorable mechanistic pathways of **5CQA**. The 6-311++G(d,p) basis set was used in all cases

Mechanism	Position	Γ (%)		
		M06-2X—CPCM		M05-2X—SMD
		Benzene	Pentyl ethanoate	Benzene
$HO^{\bullet}$				
HAT	3′	4.8	0.7	1.7
	4′	1.4	0.2	2.7
RAF	1′	~0.0	~0.0	~0.0
	2′	8.7	4.6	9.4
	3′	4.7	1.4	2.3
	4′	25.4	65.7	56.5
	5′	11.2	2.9	5.3
	6′	20.5	15.3	6.0
	7′	5.8	2.2	4.2
	8′	17.5	7.0	11.8
$CH_3OO^{\bullet}$				
HAT	3′	41.5	46.6	11.2
	4′	58.5	53.4	88.8

solvation model, because energy is highly dependent on structure, and geometry of a molecule in the gas-phase differs from that of solvated molecule. M06-2X is more robust than M05-2X [14, 24]. Bearing in mind that radical and negatively charged species participate in antioxidative processes basis set needs to add diffuse functions to all atoms, including hydrogen.

Acknowledgements This work was supported by the Ministry of Education, Science and Technological Development of Serbia, Project No 172016. The authors are grateful to Reviewer for useful suggestions regarding this work.

References

1. Sayre LM, Perry G, Smith MA (2008) Oxidative stress and neurotoxicity. Chem Res Toxicol 21:172–188
2. Liu Z (2010) Chemical methods to evaluate antioxidant ability. Chem Rev 110:5675–5691
3. Hoye AT, Davoren JE, Wipf P et al (2008) Targeting mitochondria. Acc Chem Res 41:87–97
4. Crozier A, Jaganath IB, Clifford MN (2009) Dietary phenolics: chemistry, bioavailability and effects on health. Nat Prod Rep 26:1001
5. Hertog MG, Sweetnam PM, Fehily AM et al (1997) Antioxidant flavonols and ischemic heart disease in a Welsh population of men: the Caerphilly Study. Am J Clin Nutr 65:1489–1494
6. Rimm EB, Katan MB, Ascherio A et al (1996) Relation between intake of flavonoids and risk for coronary heart disease in male health professionals. Ann Intern Med 125:384–389
7. Xu JG, Hu QP, Liu Y (2012) Antioxidant and DNA-protective activities of chlorogenic acid isomers. J Agric Food Chem 60:11625–11630
8. Wang X, Wang J, Yang N (2007) Chemiluminescent determination of chlorogenic acid in fruits. Food Chem 102:422–426
9. Prior RL, Wu X, Schaich K (2005) Standardized methods for the determination of antioxidant capacity and phenolics in foods and dietary supplements. J Agric Food Chem 53:4290–4302
10. Frankel EN, Meyer AS (2000) The problems of using one-dimensional methods to evaluate multifunctional food and biological antioxidants. J Sci Food Agric 80:1925–1941
11. Antolovich M, Prenzler PD, Patsalides E et al (2002) Methods for testing antioxidant activity. Analyst 127:183–198
12. Huang D, Boxin OU, Prior RL (2005) The chemistry behind antioxidant capacity assays. J Agric Food Chem 53:1841–1856
13. Halliwell B, Aeschbach R, Löliger J, Aruoma OI (1995) The characterization of antioxidants. Food Chem Toxicol 33:601–617
14. Galano A, Alvarez-Idaboy JR (2013) A computational methodology for accurate predictions of rate constants in solution: application to the assessment of primary antioxidant activity. J Comput Chem 34:2430–2445
15. Marković S, Tošović J (2016) Comparative study of the antioxidative activities of caffeoylquinic and caffeic acids. Food Chem 210:585–592
16. Tošović J, Marković S (2016) Structural and antioxidative features of chlorogenic acid. Croat Chem Acta 89:535–541
17. Tošović J, Marković S, Dimitrić Marković JM et al (2017) Antioxidative mechanisms in chlorogenic acid. Food Chem 237:390–398
18. Chen Y, Xiao H, Zheng J, Liang G (2015) Structure-thermodynamics-antioxidant activity relationships of selected natural phenolic acids and derivatives: an experimental and theoretical evaluation. PLoS ONE 10:1–20
19. Uranga JG, Podio NS, Wunderlin DA, Santiago AN (2016) Theoretical and experimental study of the antioxidant behaviors of 5-*O*-caffeoylquinic, quinic and caffeic acids based on electronic and structural properties. ChemistrySelect 1:4113–4120
20. Frisch MJ, Trucks GW, Schlegel HB et al (2013) Gaussian 09, Revision D.01. Gaussian, Inc., Wallingford
21. Zhao Y, Truhlar DG (2008) The M06 suite of density functionals for main group thermochemistry, thermochemical kinetics, noncovalent interactions, excited states, and transition elements: two new functionals and systematic testing of four M06-class functionals and 12 other function. Theor Chem Acc 120:215–241
22. Zhao Y, Truhlar DG (2008) Density functionals with broad applicability in chemistry. Acc Chem Res 41:157–167
23. Cossi M, Rega N, Scalmani G, Barone V (2003) Energies, structures, and electronic properties of molecules in solution with the C-PCM solvation model. J Comput Chem 24:669–681
24. Zhao Y, Schultz NE, Truhlar DG (2006) Design of density functionals by combining the method of constraint satisfaction with parametrization for thermochemistry, thermochemical kinetics, and noncovalent interactions. J Chem Theory Comput 2:364–382
25. Marenich AV, Cramer CJ, Truhlar DG (2009) Universal solvation model based on solute electron density and on a continuum model of the solvent defined by the bulk dielectric constant and atomic surface tensions. J Phys Chem B 113:6378–6396
26. Redžepović I, Marković S, Tošović J (2017) Antioxidative activity of caffeic acid—mechanistic DFT study. Kragujev J Sci 39:109–122
27. Iuga C, Alvarez-Idaboy JR, Russo N (2012) Antioxidant activity of trans -resveratrol toward hydroxyl and hydroperoxyl radicals: a quantum chemical and computational kinetics study. J Org Chem 77:3868–3877
28. Markovic Z, Amic D, Milenkovic D et al (2013) Examination of the chemical behavior of the quercetin radical cation towards some bases. Phys Chem Chem Phys 15:7370–7378
29. Medina ME, Iuga C, Alvarez-Idaboy JR (2014) Antioxidant activity of fraxetin and its regeneration in aqueous media. A density functional theory study. RSC Adv 4:52920–52932

30. Amić A, Lučić B, Stepanić V et al (2017) Free radical scavenging potency of quercetin catecholic colonic metabolites: thermodynamics of 2H +/2e − processes. Food Chem 218:144–151
31. Milenković D, Đorović J, Petrović V et al (2017) Hydrogen atom transfer versus proton coupled electron transfer mechanism of gallic acid with different peroxy radicals. React Kinet Mech Catal 123:215–230
32. Okuno Y (1997) Theoretical investigation of the mechanism of the Baeyer–Villiger reaction in nonpolar solvents. Eur J Chem 3:212–218
33. Alberty RA (1960) The foundations of chemical kinetics (Benson, Sidney W.). J Chem Educ 37:660
34. Marković Z, Tošović J, Milenković D, Marković S (2016) Revisiting the solvation enthalpies and free energies of the proton and electron in various solvents. Comput Theor Chem 1077:11–17
35. Eckart C (1930) The penetration of a potential barrier by electrons. Phys Rev 35:1303–1309
36. Duncan WT, Bell RL, Truong TN (1998) TheRate: program for ab initio direct dynamics calculations of thermal and vibrational-state-selected rate constants. J Comput Chem 19:1039–1052
37. Fernández-Ramos A, Miller JA, Klippenstein SJ, Truhlar DG (2006) Modeling the kinetics of bimolecular reactions. Chem Rev 106:4518–4584
38. Alberto ME, Russo N, Grand A, Galano A (2013) A physicochemical examination of the free radical scavenging activity of Trolox: mechanism, kinetics and influence of the environment. Phys Chem Chem Phys 15:4642
39. Medina ME, Iuga C, Álvarez-Idaboy JR (2013) Antioxidant activity of propyl gallate in aqueous and lipid media: a theoretical study. Phys Chem Chem Phys 15:13137
40. Marino T, Russo N, Galano A (2016) A deeper insight on the radical scavenger activity of two simple coumarins toward OOH radical. Comput Theor Chem 1077:133–138
41. Dimić DS, Milenković DA, Marković JMD, Marković ZS (2017) Thermodynamic and kinetic analysis of the reaction between biological catecholamines and chlorinated methylperoxy radicals. Mol Phys 8976:1–13
42. Galano A, Tan DX, Reiter RJ (2011) Melatonin as a natural ally against oxidative stress: a physicochemical examination. J Pineal Res 51:1–16
43. Rose RC, Bode AM (1993) Biology of free radical scavengers: an evaluation of ascorbate. FASEB J 7:1135–1142